ACS APPLIED MATERIALS & INTERFACES

Research Article

Cite This: ACS Appl. Mater. Interfaces XXXX, XXX, XXX−XXX

www.acsami.org

Magnetic Responsive PVA Hydrogels for Remote Modulation of Protein Sorption

Ana C. Manjua,[†,‡] Vitor D. Alves,[§] João G. Crespo,[†] and Carla A. M. Portugal*[,†]

[†]LAQV-Requimte, FCT-Universidade Nova de Lisboa, Campus da Caparica, 2829-516 Caparica, Portugal

[‡]Department of Bioengineering and iBB-Institute for Bioengineering and Biosciences, IST-Universidade de Lisboa, Av. Rovisco Pais, 1049-001 Lisboa, Portugal

[§]LEAF-Linking Landscape, Environment, Agriculture and Food, Instituto Superior de Agronomia, Universidade de Lisboa, Tapada da Ajuda, 1349-017 Lisboa, Portugal

Supporting Information

ABSTRACT: This work shows the ability to reversibly modulate the hydrophilicity of the hydrogels doped with iron oxide nanoparticles (MNPs) in a noninvasive way when exposed to a cyclic variation of the intensity (ON/OFF) of an external magnetic field. A reversible switching of surface contact angles was observed for magnetic PVA hydrogels when exposed to consecutive variation of the magnetic field intensity between 0 and 0.08 T. Motivated by the magnetic dependence of the hydrophilicity of these hybrid hydrogels, the impact of the magnetic field on protein sorption was also evaluated. The noninvasive regulation of protein sorption-released mechanisms was achieved by ON/OFF magnetic field switches, suggesting the possible influence of magnetic-induced hydrogel shrinking effect and changes of surface wettability on protein sorption. The capacity to magnetically modulate surface wettability and protein sorption make these magnetic hydrogels promising candidates for development of functional devices for tissue engineering, drug release applications, or biosensor systems, where the control of protein sorption and mobility are essential steps to improve the efficiency of these processes.

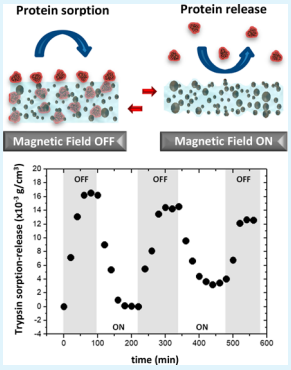

KEYWORDS: *ferrogel, magnetic field, protein sorption, surface topography, membrane wettability*

1. INTRODUCTION

Protein−surface interactions exert a paramount role in the control of bioprocess performance. Nonspecific adsorption of proteins promotes the uncontrolled accumulation of these molecules at surfaces leading to undesirable biofouling events,[1−3] rendering processes with low efficiencies due to hindered molecular transport through the processing media. Besides the prejudicial effect of biofouling, the structural behavior of proteins at surfaces has an important influence in molecular recognition mechanisms, as those inherent to affinity-based separations processes,[4] biosensors,[5,6] and regenerative medicine systems.[7,8] Protein−surface interactions are generally followed by changes of protein conformation whose amplitude depends on the surface and protein properties. Protein structural deformation at surfaces not only affects protein binding stability but also may generate higher or lower exposure of important epitopes (binding sites or molecular recognition peptide segments), thus ruling the accessibility of target solutes (e.g., enzymatic substrates and cells) to specific protein binding sites.

The ability to control protein behavior at surfaces is thus an essential aspect in bioprocessing[9] and different regenerative medicine issues, e.g., tissue engineering, organ implants, wound healing, and (bio)artificial organs. The accessibility of transmembrane cell receptors (e.g., integrins) to specific peptide binding sequences (e.g., RGDS) contained in adhesion proteins at the tissue scaffold is a determinant for the development of cell tissue. The intensity of cell adhesion defines the cell stability and density at scaffolds as well as the force balance established between the cytoskeleton and the scaffold which are primary activators of cell signaling mechanisms driving cell differentiation into tissues with desirable phenotypes.[10] In contrast, the development of surfaces exhibiting minimal protein adsorption remains as a major challenge in the design of implants and (bio)artificial organs with improved biocompatibility.[11] The adsorption of blood proteins (immunoglobulins) and their structural unfolding at surfaces are promoters of immune responses (e.g., complement activation), which may result in uncontrolled inflammation processes ending up in the rejection of the foreign body (e.g., implants) by the host (e.g., patients).[12] Additionally, protein adsorption at surfaces prompts the formation of aggregates, which may cause the disruption of blood circulation increasing the risk of thrombosis.

Functional surfaces with tailored topographies and chemistries have been designed aiming to reduce protein adsorption while controlling their conformation at surfaces[13] to obtain a better control over molecular interfacial events. Both protein

Received: February 19, 2019
Accepted: May 14, 2019

DOI: 10.1021/acsami.9b03146
ACS Appl. Mater. Interfaces XXXX, XXX, XXX−XXX

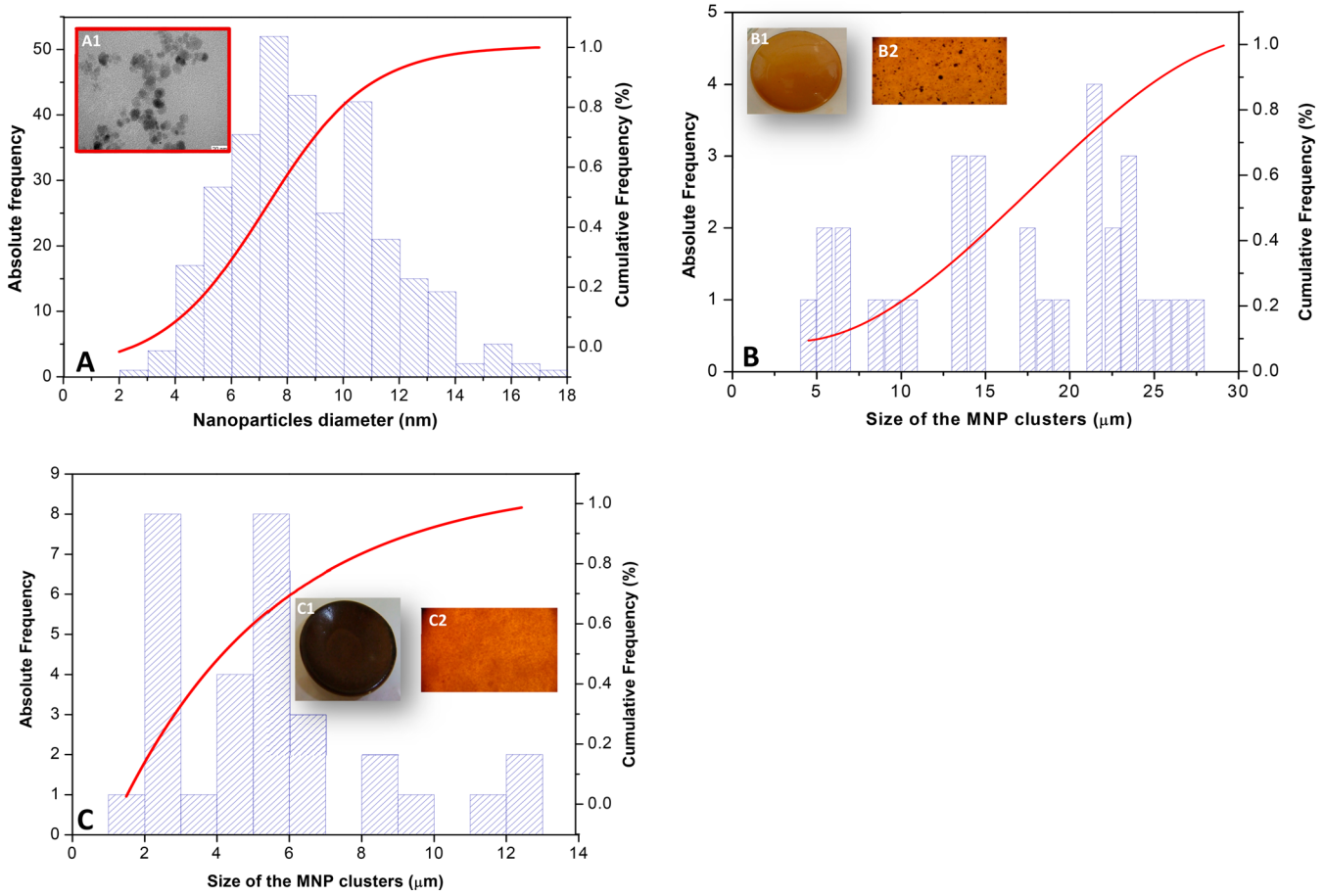

Figure 1. Size distribution of the (A) magnetic nanoparticles (MNPs) obtained by ImageJ treatment of TEM analysis, (B) MNP clusters in PVA hydrogels doped with 0.25% of MNPs, and (C) MNP clusters in PVA hydrogels doped with 1% of MNPs, obtained by ImageJ treatment of the optical microscopy images. Relative and cumulative frequencies are represented by the bars and the red line, respectively. Insets: (A1) TEM image of the MNPs. Photos (B1 and C1) and optical microscopy images (B2 and C2) of PVA hydrogel membranes doped with 0.25% and 1% MNPs, respectively.

adsorption capacity and structural behavior at surfaces are intimately related to surface hydrophilic/hydrophobic degree.[14−16] Hence, most surface functionalization strategies have involved the design of surfaces with tailored static[17,18] or dynamic wettability (stimuli-responsive surfaces),[14,19,20] envisaging the development of antifouling surfaces or materials with improved biocompatibility, by the reduction of protein adsorption. In accordance with the Wentzel[21] as well as Cassie and Baxter[22] models, the surface wettability is influenced by the surface topography, i.e., surface roughness. Surface roughness is described to play a key role in modulating cell behavior for implant biomaterials (e.g., titanium, ceramics, stainless steel, and polymers).[23] Roughness enhances the hydrophilic degree of surfaces with high free energy as well as the hydrophobic degree of surfaces with low free energy.[14,19,24,25] The relation between roughness and the surface hydrophilic/hydrophobic character has been exploited toward the design of responsive surfaces able to exchange between extreme hydrophilic (superhydrophilic) and hydrophobic (superhydrophobic) characters. This responsive behavior has been mostly achieved by incorporation of stimuli-sensitive molecules into surfaces with accentuated roughness.[19]

Hence, hydrophilic−hydrophobic switches are due to the reversible changes of the free energy of the stimuli-responsive agents when exposed to variable stimuli conditions, e.g., pH, temperature, or light, which are then amplified by the surface roughness. Such unique functionality has been explored toward the development of antifouling membranes and responsive tissue scaffolds envisaging an efficient modulation of cell behavior,[26,27] that is, a better organization of cell cocultures and on-demand cell detachment at/from the tissue scaffolds[28,29] based on a suitable control of protein adsorption.

Aiming to explore the beneficial effects of stimuli-responsive surfaces, the combination of the photothermal properties of nanocomposite hydrogels with magnetic ability has been demonstrated to function as a heating source with controlled position and location of healing through a magnet for potential applications such as drug delivery, controlled catalysis, and microdevices.[30] External high-frequency alternating current electric fields can also be used to promote direct assembly of hard colloidal particles into linear chains and clusters within a soft thermoresponsive pNIPAAM hydrogel membrane to perform catalytic roles or function as tissue adhesives, artificial cartilage, and sensors.[31]

Thermoresponsive properties of pNIPAAM have also been explored toward the design of membranes which based on the swelling−unswelling mechanisms of pNIpAAM around the low critical solution temperature (LSCT) are capable of a reversible adjustment of pore sizes allowing for a better control of the permeate fluxes, solute permeation[32] and protein

DOI: 10.1021/acsami.9b03146
ACS Appl. Mater. Interfaces XXXX, XXX, XXX−XXX

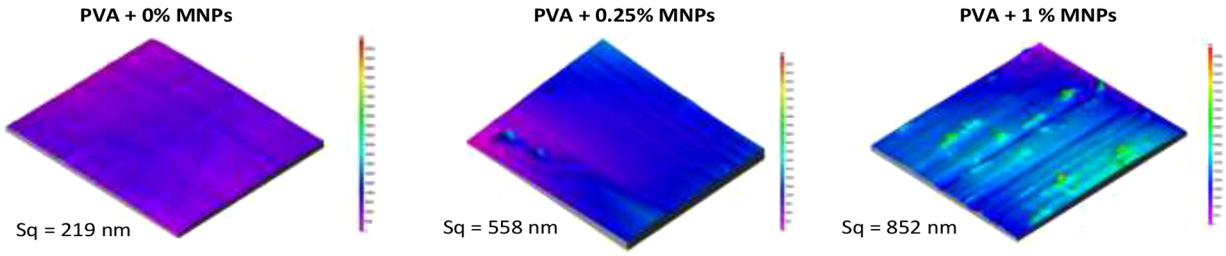

Figure 2. Profilometry images of PVA hydrogels and their respective surface roughness, *Sq*.

binding.[33] Furthermore, pH responsive polymeric membranes have been reported with the ability to reversibly enhance mass transport by increasing the flux more than 2 orders of magnitude when switching the pH from 2 to 8.[34]

However, the use of these responsive systems modulated by addition of mass agents, e.g., pH, is undesirable in most applications, since they involve the consecutive accumulation of the agents responsible for inducing the surface response. Likewise, the use of temperature responsive surfaces is limited to thermal insensitive processes whereas photoresponsive behaviors are mostly ruled by slow reversible photoisomerization reactions, leading to delayed responses or losses of responsive capacity.

Magnetic responsive soft polymers, e.g., hydrogels, and integrating magnetic nanoparticles (MNPs), such as iron oxide nanoparticles, have been shown to be able to respond to an adequate magnetic field in a fast mode, with reversible changes of their shape and volume.[35,36] For instance, the direct incorporation of covalently attached metal nanoparticles/nanomagnets into the backbone of a hydrogel allows for the design of significantly stronger magnetic actuators with higher mechanical stability, muscle-like flexibility, and shape memory effect with potential for their use in tissue engineering as soft actuators or artificial muscles.[37,38]

Contraction−distension of these hydrogels is driven by the movements of the embedded MNPs induced by magnetic attractive−repulsive forces imposed by a nonuniform magnetic field.[35] Profiting from their magnetically driven shrinking−unshrinking ability, these hybrid assemblies have been applied as mechanical actuators, used for the design of membranes with adjustable pore sizes,[39] as activators of molecular motors to mimic nature systems,[40] and to modulate cell responses at magnetic responsive hydrogel scaffolds.[41,42] Magnetic hydrogels were shown to provide a means to remotely induce mechanical forces with controlled direction and intensity, similar to that required for cell mechanotransduction (∼1 pN).[41] This magnetomechanical stimulation was showed to elevate the metabolic activity of aortic endothelial and cardiac cells in the presence of an alternating current (ac) magnetic field ascribed to an accurate magnetic control of cellular organization.[41] In a different work from Tognato et al.,[42] magnetic responsive hydrogels with anisotropic alignment of MNPs were shown to be able to induce the differentiation of C2C12 myoblasts into myotubes in the absence of differentiation media.

This work reports the ability to regulate the sorption and release of proteins at PVA hydrogel with embedded magnetic nanoparticles, taking advantage of the magnetic responsive ability of these materials. These studies were performed to understand the impact of the magnetic response of these hydrogels on protein sorption and release aiming to elucidate about their potential contribution for development of tissue engineering, drug release, or biosensing systems with improved efficiency.

2. RESULTS AND DISCUSSION

Magnetic Responsive Behavior of the Hydrogel Membranes. Magnetic sensitive hydrogel membranes with isotropic magnetic morphology were obtained by random dispersion of iron oxide nanoparticles (MNPs), with sizes ranging from 2 to 20 nm and an average diameter of ∼9 nm (Figure 1A), in poly(vinyl alcohol) (PVA) solution. PVA membranes with physically entrapped iron oxide nanoparticles (MNPs) were formed upon cross-linking of the PVA chains using glutaraldehyde (GA). The GA fraction added was such to confer a good structural stability and robustness to the membrane matrix, avoiding particle displacement and coalescence, with minimum detriment of the surface elasticity. These hybrid hydrogel membranes exhibited magnetic architectures, formed by randomly well-dispersed micro-MNP clusters (Figures S1 and S2 in the Supporting Information) of heterogeneous sizes. As shown in Figures 1B and 1C, the hydrogels doped with 0.25% of MNPs exhibit MNP clusters, with sizes varying from 3 to 28 μm and an average size of 16.7 ± 7.0 μm, whereas hydrogels doped with 1% MNPs showed lower sized clusters with dimensions varying between 2 and 12 μm and an average size of 5.6 ± 2.8 μm. These hydrogels were characterized regarding their magnetic properties by determination of their saturation magnetization curves (Figure S3). A comparative analysis of the magnetization saturation curves showed an increase of the magnetic saturation from 0.031 to 0.192 emu/g due to the increase in the concentration of MNPs from 0.25% to 1%. The absence of hysteresis loops confirmed that both PVA hydrogels with 0.25% and 1% MNPs have a typical superparamagnetic behavior, without remanent magnetization upon removal of the magnetic field.[43]

The impact of the MNP clusters on the surface roughness of the hydrogels was also studied by profilometry analysis. The profilometry images in Figure 2 showed an increase of the surface roughness from 219 to 852 nm, as the MNP content increased from 0% to 1%.

However, considering the magnetic susceptibility of the MNPs and assuming that entrapped MNPs can still move due to the elasticity of the hydrogel, one may hypothesize a potential influence of the magnetic field on the surface texture of PVA hydrogels (e.g., roughness). Taking into account the relationship between the surface roughness and the hydrophilic−hydrophobic character as expressed by the Wentzel and Cassie−Baxter theories,[19,20] the magnetic dependence of the surface properties was inspected by determining the impact of the magnetic field on the surface contact angle. Analyses of the

DOI: 10.1021/acsami.9b03146
ACS Appl. Mater. Interfaces XXXX, XXX, XXX−XXX

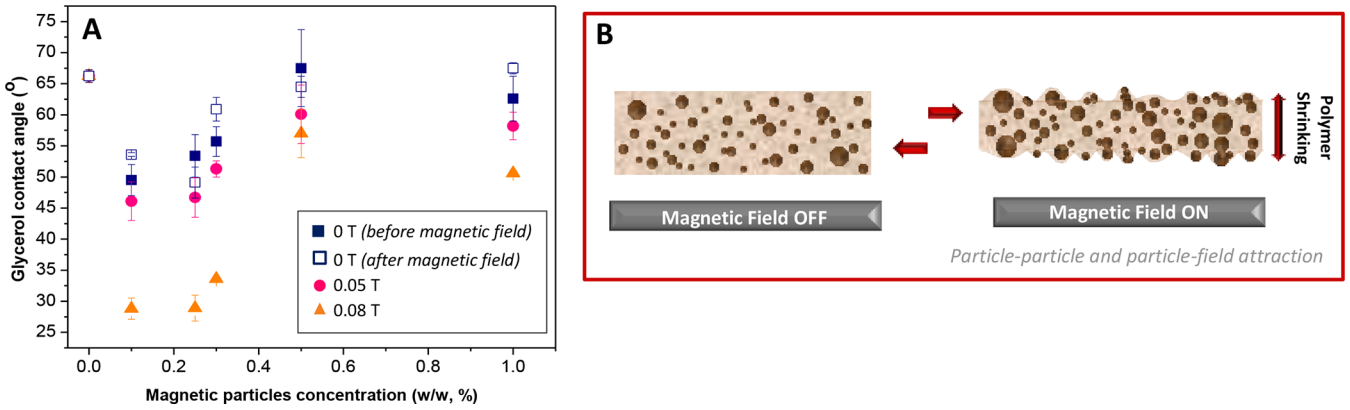

Figure 3. (A) Impact of the magnetic field on the glycerol contact angle at the surface of nonmagnetic and magnetic hydrogels doped with different concentration of MNPs. (B) Schematic representation of the magnetic induced reversible roughness of the hydrogel surface.

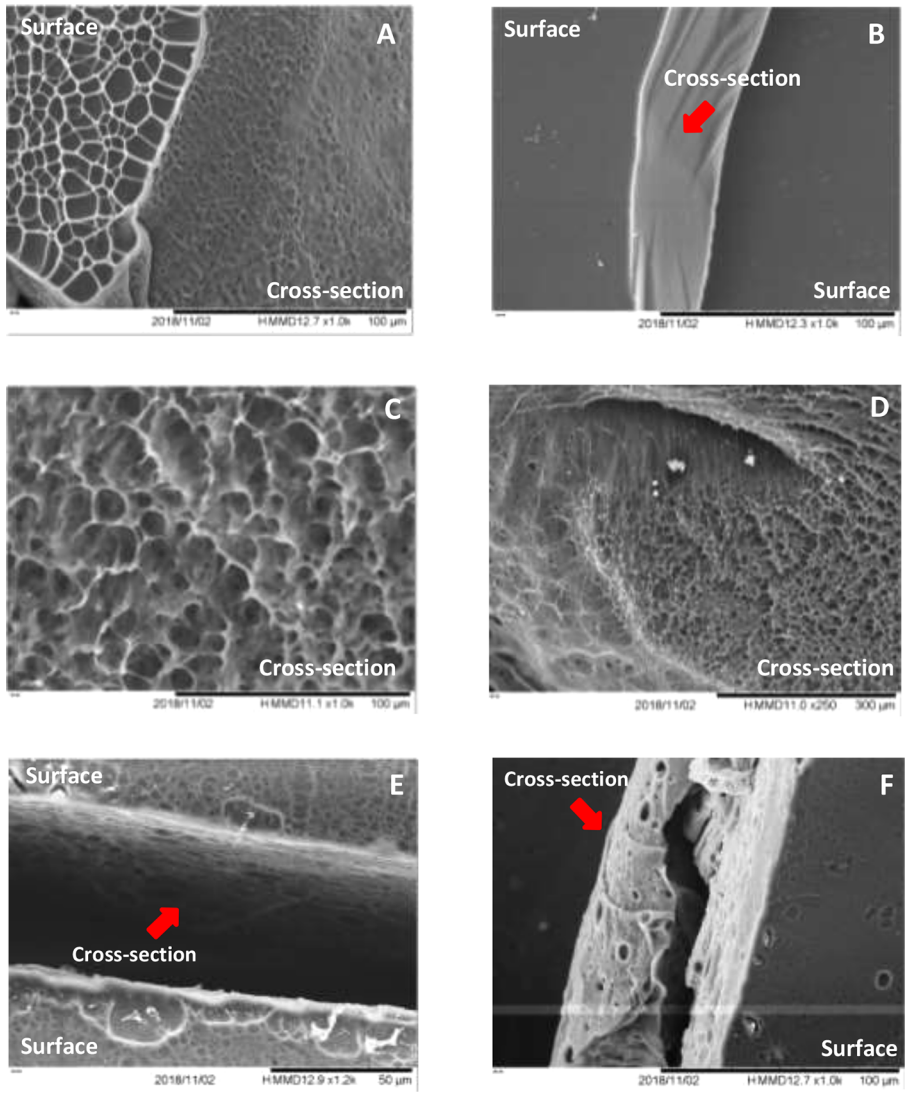

Figure 4. Environmental SEM (ESEM) images of surfaces and cross sections of nonmagnetic PVA hydrogel membrane (A, H_2O saturated; B, dry) and PVA hydrogel membrane with (C, D) 0.25% MNPs and (E, F) 1% MNPs before exposure to the magnetic field.

surface contact angle (CA) were performed using glycerol as the solvent in the absence and presence of a nonuniform magnetic field. The magnetic field was applied by placing a neodymium bar underneath the membrane, whereas the magnetic field intensity was varied from 0 to 0.08 T by adjusting the distance between the neodymium magnet and the membrane.

As shown in Figure 3A, the values of the contact angles obtained for the magnetic hydrogel membranes with MNP loads up to 1% were shown to decrease proportionally to the

DOI: 10.1021/acsami.9b03146
ACS Appl. Mater. Interfaces XXXX, XXX, XXX−XXX

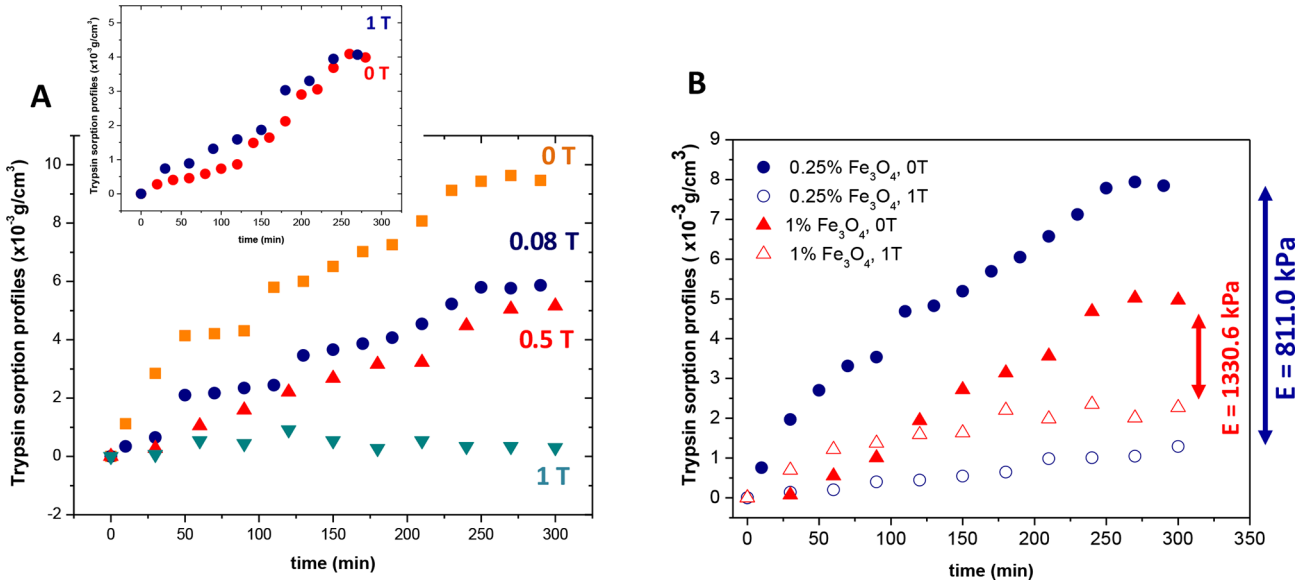

Figure 5. (A) Time-dependent trypsin sorption at magnetic hydrogel surfaces doped with 0.25% (w/v) of MNPs under different magnetic field intensities. Inset: influence of magnetic field on the tryspin sorption at surfaces of nonmagnetic hydrogels at 0 and 1 T. (B) Trypsin sorption observed at hydrogel surfaces with 0.25% (w/v) and 1% (w/v) of MNPs at 0 and 1 T, respectively, and Young's modulus, *E* (kPa).

magnetic field intensity. Thus, the contact angle of hydrogel membranes with 0.25% MNPs, which showed an initial value of 53° at 0 T, decayed to 46° at 0.05 T and to 28° at 0.08 T. Also, the effect of the magnetic field on the contact angles was found to depend on the MNPs load in the hydrogel. The highest contact angle decay was observed for hydrogels with lower MNP amounts. Hydrogels doped with 0.25% MNPs showed a contact angle decay of ca. 25° at 0.08 T, whereas a decrease of only 14° was achieved for hydrogels with 1% MNPs at the same magnetic field intensity. On the basis of these results, a higher effect would be expected if higher magnetic field intensities were applied; however, the determination of surface contact angles at stronger magnetic fields was impaired by the impossibility to couple the drop shape analysis system used for the determination of the contact angles to powerful magnetic field sources, e.g., an electromagnet system.

To clarify the role of MNPs in the hydrogels magnetic response, the impact of magnetic field on hydrogels without MNPs was also inspected. As shown in Figure 3A, the contact angles of hydrogel membranes without MNPs remained invariable, not depending on the magnetic field conditions (noticeable by the overlapping of the data points obtained for hydrogels with 0% MNPs exposed to different magnetic field intensities, Figure 3A). This result confirms that the magnetic responsive behavior of these hydrogels was exclusively due to the magnetic susceptibility of the MNPs.

Because no chemical modifications were expectable due to the magnetic field, changes of the surface contact angles should be interpreted as a consequence of structural alterations taking place in hydrogel matrix when exposed to the magnetic field. These structural changes are thought to result from a synergistic effect of the magnetic susceptibility of the embedded MNPs and the elasticity of these hybrid membranes. Despite their physical entrapment within the hydrogel membranes, MNPs may still be able to move in response to particle−particle and particle−field forces imposed by the applied magnetic field. The MNP mobility induced by the magnetic field is allowed by the elasticity of the hydrogel matrix, leading to the structural deformation of the hydrogel. A schematic illustration of the possible deformation of PVA hydrogels when exposed the magnetic field perpendicularly oriented toward the hydrogel surface is shown in Figure 3B. According to this scheme, when the magnetic field is applied, the MNPs are attracted to each other and according to the magnetic field leading to the hydrogel shrinking. This hypothetical interpretation is in total agreement with the studies developed by Szábo et al.[35] and Snyder et al.,[36] which showed the ability of ferrogels to undergo volume and shape changes, leading to hydrogel volume shrinking in the presence of magnetic field. In this case, it is plausible to think that membrane shrinking might bring a higher amount of MNPs closer to the membrane surface, leading to an increase of the surface roughness followed by an increase of the surface wettability. It is important to highlight that since Fe_3O_4 particles (MNPs) exhibit size-dependent saturation magnetization,[44] the presence of some MNP clustering observed in the hydrogels is expected to exert a beneficial effect on the magnetic responsive capacity of these hybrid hydrogels. Despite being plausible, this explanation should be considered as a hypothetical interpretation given the impossibility to have a direct measurement of the hydrogel surface roughness in the presence of a magnetic field.

Differences in the intrinsic porous structure (in the absence of magnetic field) of hydrogels doped with different amounts of MNPs may, however, explain the lower surface contact angles observed for hydrogels with lower MNP contents, i.e., <0.25% (Figure 3A). This effect was supported by analysis of swollen hydrogels with different MNP loads by environmental scanning electron microscopy (ESEM), which showed that the porosity of PVA hydrogels doped with 0.25% of MNPs (Figure 4C,D) was higher than that exhibited by PVA hydrogels without MNPs (Figure 4A) or with higher MNP contents, e.g., 1% (Figure 4E,F).

Independently of the reason underlying the magnetic behavior of the surface contact angles, it is important to note that the initial surface contact angles were promptly recovered upon removal of the magnetic field (compare filled and empty

DOI: 10.1021/acsami.9b03146
ACS Appl. Mater. Interfaces XXXX, XXX, XXX−XXX

square symbols in Figure 3A), showing that these hybrid hydrogel membranes allowed for fast and reversible response to the magnetic field.

Impact of the Magnetic Behavior of Hydrogel Membranes on Protein Sorption. Surface properties, like roughness and wettability, define the nature of protein−surface interactions[45] which is a critical aspect in the performance of tissue engineering processes, bioseparations, or biosensors, whose efficiency is highly dependent on protein attachment ability/stability, mobility, and structural dynamics at interfaces. In this sense, studies were performed aiming to evaluate the potential use of magnetic responsive hydrogel membranes for the modulation of protein sorption (adsorption and absorption) to contribute to improving the performance of bioprocesses.

At this point, the readers should bear in mind that protein sorption considers both (i) protein adsorption, which results from the attachment of the proteins at the external and internal hydrogel surfaces, and (ii) protein absorption, which is due to the diffusion of the protein molecules in solution into the hydrogel matrix. Protein adsorption and absorption processes were difficult to distinguish in the experimental conditions used in the present work. Thus, the individual effect of magnetic field on protein adsorption and absorption is not shown but discussed in terms of protein sorption.

Protein sorption studies were developed in the absence and presence of magnetic field oriented perpendicularly to the hydrogel surfaces doped with 0.25% and 1% MNPs, using trypsin as a model protein. Trypsin sorption profiles obtained at different magnetic field intensities (up to 1 T) are shown in Figure 5A. The analysis of these profiles showed that the amount of trypsin in the membrane decreases proportionally to the magnetic field intensity, evidencing that the magnetic field reduces protein sorption ability. In fact, the amount of trypsin sorbed, after 250 min, when exposed to a constant magnetic field intensity of 1 T is insignificant when compared to the 9×10^{-3} g/cm^3 sorbed, during the same time in the absence of magnetic field.

The impact of the magnetic field on trypsin sorption in hydrogels without MNPs was also evaluated. As shown in the inset of Figure 5A, the trypsin sorption profiles obtained at 0 and 1 T were similar, confirming that the magnetic-induced variation of protein sorbed in the magnetic hydrogel membranes was actually ascribed to the magnetic responsive behavior of the hydrogels and not to a potential intrinsic magnetic sensitivity of trypsin.

As mentioned previously, the decrease of protein sorption in the presence of magnetic field should thus be deconvoluted in the two sorption components, i.e., the decrease of protein adsorption and absorption. Therefore, assuming that both processes are present, the decrease of protein absorption may correspond to a hindered diffusion of trypsin into the porous membrane structure caused by the shrinkage of the hydrogel volume when the magnetic field is applied. Instead, the decrease of protein adsorption at hydrogel membranes in the presence of magnetic field might be explained by the lower protein adsorption stability at hydrophilic surfaces.

The effect of the MNP content in the magnetic responsiveness of the hydrogel membranes was also investigated by a comparative analysis of the trypsin sorption profiles obtained for hydrogels with 0.25% and 1% MNPs at 0 and 1 T. As depicted in Figure 5B, the difference between the protein sorbed in the absence and presence of the magnetic field was higher in hydrogel membranes with 0.25% MNPs. These results are in agreement with the effect of the magnetic field on the contact angles discussed above and confirm the higher magnetic responsiveness of hydrogel membranes with lower MNP content as well as their higher ability to magnetically modulate protein sorption. The higher magnetic responsiveness of hydrogels with lower MNP content may be related to the lower resistance to deformation of these hydrogels, which was confirmed by puncture tests. The higher resistance to deformation of hydrogels with higher MNP load was expressed by the increase of the Young modulus, E, from 811.0 ± 253.4 to 1330 ± 59.6 kPa when the concentration of MNPs increased from 0.25% to 1%. On the basis of these results, it is reasonable to think that hydrogels with high elasticity allow for higher levels of hydrogel volume contraction due to an easier mobility of the embedded MNPs, thus explaining their higher magnetic responsiveness. This result further suggests that the optimization of the magnetic responsiveness of these hydrogels relies on a good balance between the MNP load (high enough to ensure the magnetic responsiveness of the hydrogel) and the resultant increase of the hydrogel resistance to deformation (low enough to allow the magnetic mobility of the MNPs entrapped in the hydrogel matrix).

Control of Protein Sorption in Hydrogel Membranes under Cyclic Magnetic Field Conditions. Studies about the impact of the magnetic field on the trypsin sorption profiles in the hydrogel membrane were also performed under cyclic variation of the magnetic field intensity between 0 T (magnetic field OFF) and 1 T (magnetic field ON) to evaluate the process reversibility. As shown in Figure 6A, the amount of trypsin in the membrane increased along the first stage when the magnetic field was OFF. When the trypsin sorption plateau was reached, the magnetic field was switched ON at 1 T, and a fast displacement of trypsin back to the supernatant solution was observed corresponding to the release of 61.8% (Table S1) of the total amount of the protein in the membrane. The trypsin sorption into the hydrogel membrane was immediately restored when the magnetic field was switched OFF (second cycle). However, not only the protein sorption plateau reached in the second magnetic field cycle was higher but also the efficiency of the protein release decayed to 7.1%, suggesting a loss of the magnetic responsive capacity of the membrane and the accumulation of protein in the hydrogel matrix. The amount of trypsin sorbed and released at each magnetic field stage was calculated by a mass balance shown in Table S1. It is important to highlight that protein desorption due to thermal effects was excluded since the temperature at the surface of the hydrogels was kept constant along the process.

Additional studies were developed aiming at understanding the reasons underlying the higher protein retention (expressed by the increase of the protein sorption plateau) and the decrease of protein release capacity of the hydrogels with the number of magnetic field cycles.

Analysis of the variation of the hydrogel surface contact angles performed under identical magnetic field cycle frequency (but with a lower magnetic field intensity of 0.08 T) showed that the contact angle switching amplitude was essentially preserved along the process (Figure 6B), suggesting that the magnetically induced mechanic activity of the hydrogel membrane was maintained. Therefore, losses of protein release ability seemed not to be related to losses in the magnetic responsive capacity of the hydrogel.

DOI: 10.1021/acsami.9b03146
ACS Appl. Mater. Interfaces XXXX, XXX, XXX−XXX

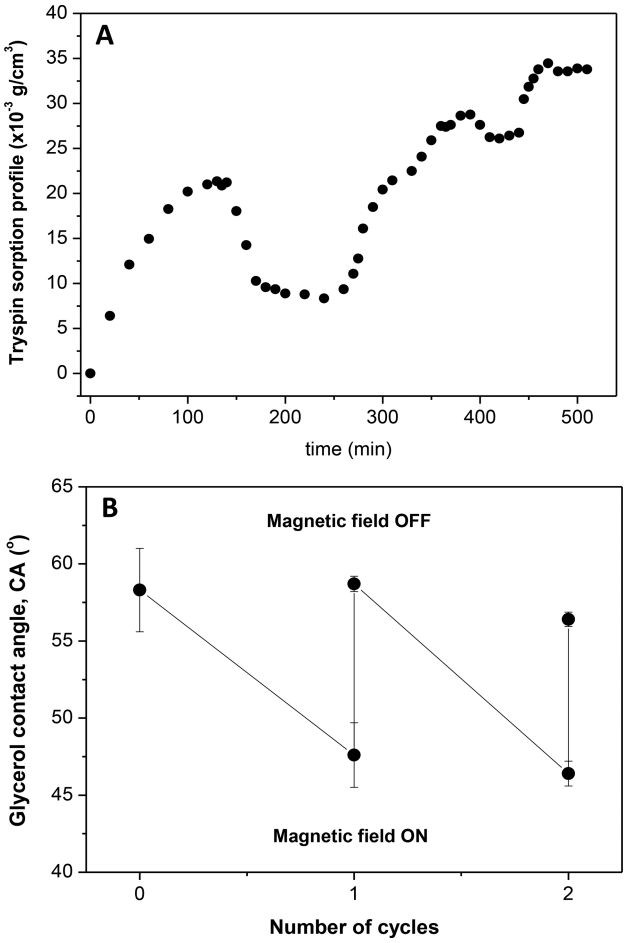

Figure 6. (A) Evolution of trypsin content along time in a PVA hydrogel membrane doped with 0.25% (w/v) of MNPs when exposed to magnetic field cycles varied between 0 and 1 T. (B) Glycerol contact angles, CA (deg), obtained along OFF/ON magnetic field cycles at 0.08 T for a magnetic hydrogel matrix with 0.25% (v/w) of MNPs upon exposure to OFF/ON magnetic field cycle at 1 T.

To confirm the protein accumulation in the hydrogel along the magnetic field cycles, the sorption studies were repeated using fluorescein isothiocyanate (FITC)-labeled albumin (FITC-albumin) instead of trypsin. Confocal microscopy images were acquired for hydrogel membranes doped with 0.25% MNPs after immersion in the protein solution in the absence (magnetic field OFF) and the presence of OFF/ON magnetic field cycles. It is important to highlight that to ensure the analysis of the hydrogel membrane was performed upon maximum protein desorption, the membrane was removed from the protein solution at the end of the ON magnetic field stage, while the magnetic field was still turned ON.

The confocal images depicted in Figure 7 confirmed the presence of protein inside the two hydrogel membranes, i.e., the membranes exposed and nonexposed to magnetic field cycles. The progressive increase of fluorescence emission from the membrane periphery to the membrane center, i.e., from $Z = 0$ to the membrane half thickness, unveiled the preferential accumulation of FITC-albumin in the membrane core. However, a comparative analysis of the confocal images obtained for the two membranes showed a lower fluorescence signal in the membrane exposed to magnetic field cycle, suggesting a partial removal of protein during the ON magnetic field stage. Also, it shows that a protein fraction remains entrapped in the hydrogel matrix, which is compatible with the progressive increase of the trypsin sorption plateau observed along the magnetic field cycles, as shown in Figure 6A.

The subsequent increase of the protein sorption maxima (i.e., protein sorption plateaus) suggests a continuous accumulation of protein in the membrane, which might be ascribed with the increase of the free volume inside the hydrogel matrix, potentially associated with the disruption of the hydrogel porous network caused by the magnetically induced mobility of the MNPs. Despite the efforts developed to confirm the presence of structural changes after exposure to the magnetic field cycles, no changes in MNP dispersion quality (Figures S1 and S2) or hydrogel porous structure (Figure S4) were noticed by optical microscopy and ESEM analysis (Figures S2 and S4).

To further clarify the reasons for the loss of protein sorption−desorption reversibility along the magnetic field cycles, protein sorption−release experiments were repeated at a lower magnetic field intensity of 0.45 T. The reduction of the magnetic field intensity aimed to induce a smoother movement of the MNPs in these conditions, thus preventing the hypothetical disruption of the hydrogel network. In this case, trypsin sorption was performed by exposing hydrogel membranes doped with 0.25% MNPs to magnetic field cycles with opposite ON/OFF sequences, i.e., OFF/ON (Figure 8 A) and ON/OFF (Figure 8 B) magnetic field sequences. The trypsin sorption profiles obtained during OFF/ON magnetic field cycles (Figure 8 A) and the respective mass balances, listed in Table S2, show that the membrane was able to release the total amount of trypsin sorbed during the first OFF/ON cycle. Although the small loss of the magnetic responsiveness observed through the subsequent magnetic field cycles (with protein sorption decaying from 32.4% to 19.4% and protein release decreasing from 100% to 76.1% after the second cycle), the magnetically induced protein sorption and release capacity of the PVA hydrogel was significant along the whole process time.

Experiments performed under ON/OFF magnetic field conditions, depicted in Figure 8B (and the respective trypsin mass balance listed in Table S.3), showed that trypsin sorption in the membrane (i.e., protein adsorption and absorption into the membrane matrix) was minimal while the magnetic field was kept ON. Then, when the magnetic field was switched OFF, an immediate increase of trypsin sorption was observed. A removal of 96.3% of the total amount of trypsin in the membrane was observed after the first magnetic field cycle whereas it decayed to 78.6% after the second cycle.

The more efficient protein release observed for experiments performed at lower magnetic field intensity (Figure 8) suggested that the accumulation of protein within the hydrogel matrix, observed when the magnetic field was increased up to 1 T, might actually be due to the presence of structural changes in the hydrogel. The mobility of the MNPs is certainly more abrupt at 1 T, causing a more significant disruption of the hydrogel porous structure and the increased protein retention capacity observed in this case (Figure 7). Instead, the protein sorption and release behavior observed at 0.45 T suggests that the membrane structure is more likely preserved at lower magnetic field intensities, allowing for a more efficient and reproducible magnetic responsive behavior.

Magnetically induced changes of the hydrogel structure may explain both the decrease of protein adsorption and absorption

DOI: 10.1021/acsami.9b03146
ACS Appl. Mater. Interfaces XXXX, XXX, XXX−XXX

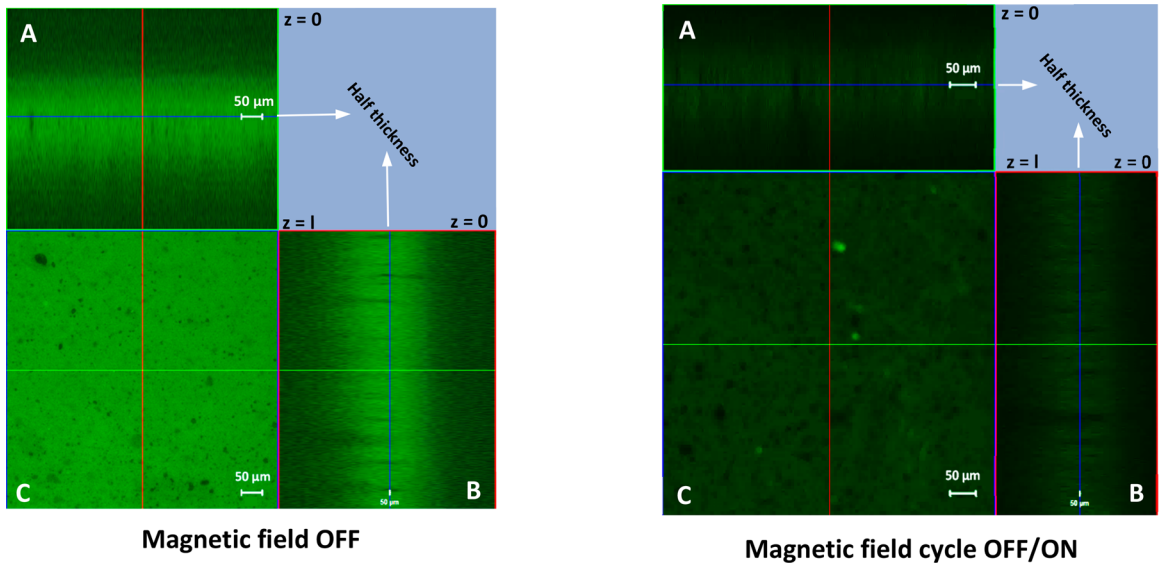

Figure 7. Confocal microscopy orthogonal images obtained along the *Z*-axis (thickness, from *Z* = 0 to *Z* = l) of a magnetic hydrogel membrane with 0.25% (v/w) MNPs upon immersion in a solution of FITC-albumin in the absence of magnetic fied and exposed to an OFF/ON magnetic field cycle. (A) Fluorescence emission signal obtained along the whole membrane thickness (*Z* = l), (B) fluorescence emission signal obtained along the whole membrane thickness orthogonal to the side represented in (A), and (C) microscopy image obtained at the half-thickness of the membrane.

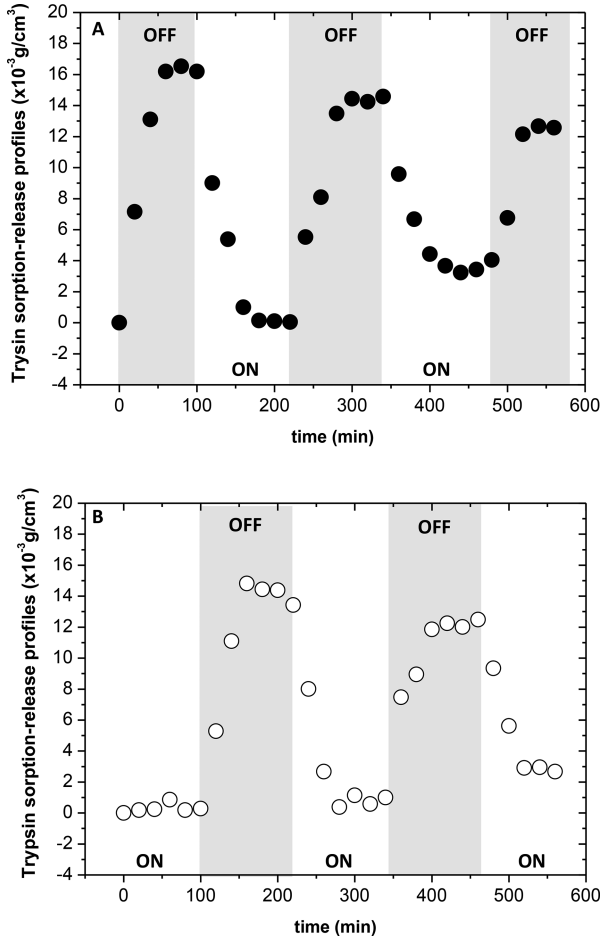

Figure 8. Evolution of trypsin sorption in a PVA hydrogel membrane doped with 0.25% (w/v) of MNPs when exposed to (A) OFF/ON and (B) ON/OFF magnetic field cycles varied between 0 and 0.45 T.

if the two processes were assumed to coexist. Protein adsorption is known to depend on surface hydrophilicity decreasing as the surface hydrophilicity increases. Hence, the lower protein partitioning to the hydrogel in the presence of magnetic field might be explained by variation of the surface hydrophilic degree imposed by the ON/OFF magnetic field cycles, with protein adsorption increasing at magnetic field OFF (decrease of the surface hydrophilicity) and decreasing at magnetic field ON (increase of surface hydrophilicity). Also, the decrease of protein sorption at the ON magnetic field stage might be ascribed with the hampered diffusion of proteins (and the protein solution), which might be related to the reduction in the hydrogel free volume caused by the magnetic hydrogel shrinking effect. Hydrogel shrinking−unshrinking is thought to emulate the peristaltic pumping effect, resulting in a higher amount of proteins inside the unshrunk hydrogels followed by protein released induced by hydrogel contraction.

3. CONCLUSIONS

This work describes the impact of magnetic field on the wettability of PVA hydrogels doped with iron oxide nanoparticles (MNPs) and the ability to modulate, in remote mode, protein sorption to these magnetic hydrogel membranes by adjustment of the intensity of an external magnetic field. The magnetic field was shown to induce a decrease of the surface contact angles of PVA hydrogels, thus suggesting an increase of surface wettability. Surface wettability responds reversibly to ON/OFF magnetic field cycles with a total recovery of the initial surface contact angles upon removal of the magnetic field. The magnetic behavior of these hydrogels was also shown to influence protein sorption. The magnetic field was shown to reduce protein sorption ability while stimulating protein release from the hydrogel. Therefore, these hydrogels offered the capacity to magnetically control the protein content by cyclic variation of the magnetic field intensity. Still, this process seems not to be totally reversible due to the partial accumulation of protein into the hydrogel matrix, particularly

DOI: 10.1021/acsami.9b03146
ACS Appl. Mater. Interfaces XXXX, XXX, XXX−XXX

evident when a magnetic field of 1 T was used. The degree of reversibly of protein sorption−desorption processes was found to be improved by decreasing the magnetic field intensity to 0.45 T.

The unique properties of these magnetic responsive hydrogels suggest their promising use as smart devices which may offer a better control over the partitioning and mobility of proteins to/in porous media. Hence, they may contribute to the development of bioseparation systems with improved performances, e.g., less prone to biofouling, and to the design of magnetically controlled drug delivery systems, biosensors, and tissue engineering devices with better efficiencies.

4. EXPERIMENTAL SECTION

Materials. $FeCl_3 \cdot 6H_2O$, $FeCl_2 \cdot 4H_2O$, potassium oleate, Hitenol-BC, and ammonium persulfate were purchased from Sigma-Aldrich, whereas 25% aqueous ammonium solution was acquired from Fluka. Poly(vinyl alcohol) (PVA), glycerol, glutaraldehyde (GA), chloride acid (HCl) solution (37%), and FITC-albumin were supplied by Sigma-Aldrich.

Synthesis of the Magnetic Nanoparticles (MNPs). The magnetic nanoparticles (MNPs) were synthesized by chemical coprecipitation of two different iron salts $FeCl_3$ and $FeCl_2$ in alkaline media according to the protocol previously published by Olle et al.[46] Briefly, an aqueous solution with 25% of ammonium hydroxide (NH_4OH) was added to a mixture of $FeCl_3$ and $FeCl_2$ at 80 °C, under permanent stirring at 1250 rpm by purging N_2. Potassium oleate and ammonium persulfate were then added to the reaction mixture for production of Fe_3O_4-coated particles aiming to minimize particle aggregation. Hitenol-BC was used as a surfactant.

Preparation of the Magnetic Responsive Hydrogel Membranes. MNPs were dispersed by sonication in an 8% PVA aqueous solution, containing 1% glycerol. 3% of GA (cross-linking agent) and 3% of HCl were added to the solution before casting onto glass plates. Magnetic responsive PVA hydrogel membranes containing different concentrations, up to 1% (w/v), of randomly dispersed MNPs were prepared. The magnetic loaded polymer solution was casted into a casting plate with a volume (mL)/casting plate area (cm^2) ratio of 0.42 mL/cm^2, which allowed for the preparation of matrices with a thickness of ca. 250 μm.

Prior to use, the magnetic PVA hydrogel membranes were washed by immersion in a demineralized water bath. The removal of nonbound material upon swelling of PVA membrane in water was followed by UV−vis spectrometry of the washing solution along time. The wash-out of magnetic particles was inspected through determination of the iron content in the washing solution by analysis of the UV band at 252 nm and by inductively coupled plasma (ICP-AES) after sample digestion. Removal of MNPs was observed during the first 3 h of washing, revealing that after this washing time hydrogels achieve good chemical and structural stability in aqueous media.

Structural Characterization of the MNPs and Hydrogel Membranes. The MNP size distribution was accessed by transmission electron microscopy (TEM) using a TEM Hitachi H8100 with a LAB6 filament and an acceleration tension of 200 kV. The MNP sizes were determined by using the ImageJ software, whereas the average particle size was elicited by statistical analysis of a total of 320 counts and using a confidence level of 95%. The dispersion quality of the MNPs was inspected by optical microscopy using a microscope (Olympus BH-2) equipped with a photo camera (Casio Exilim Pro, EX-F1) and by scanning electron microscopy using FEG-SEM equipment (JEOL, model JSM7001F) coupled to a light energy EDS detector (Oxford, model INCA 250).

The surface and cross section of hydrogel membranes with MNPs contents ranging from 0% (without MNPs) to 1% MNPs were characterized in swollen state by environmental SEM (ESEM) upon being frozen at −20 °C to minimize structural changes along the measurements due to dehydration. In contrast to conventional SEM analysis, ESEM does not require the precoating of the sample allowing analysis of the structure of swollen membrane hydrogel. Identical ESEM analyses were conducted for hydrogel membranes doped with 0.25% MNPs, before and after exposure to the magnetic field. ESEM analyses were performed using a tabletop microscope (Hitachi, TM3030Plus).

Young's Modulus of the Magnetic Hydrogel. The Young's modulus, E (kPa), of the hybrid hydrogel membranes was calculated based on the slopes of the stress−strain curves in the elastic region under puncture tests. The puncture tests were performed using a texturometer (TA-XT2 Stable Micro System, UK) equipped with a 2 mm diameter cylindrical probe, which punctured PVA hydrogels with different concentrations of MNPs (2 × 2 cm^2) at a cross-head speed of 0.5 mm/s. The values of the Young's modulus corresponded to the average values of at least three replicates.

Surface Roughness of the Hydrogel. The determination of surface roughness was initially attempted by atomic force microscopy (AFM) analysis. However, the dimension of the roughness details presented at the membrane surfaces with higher magnetic load exceeded the analytical range of this technique. For this reason, surface roughness measurements were performed by profilometry using an Ambios XP-200 profilometer equipped with a 2.5 μm tip by sequentially measuring profile lines with a 10 μm spacing and using TrueMap software for 3D images compilation. Profilometry measurements were performed using PVA membranes in their maximum swollen state, attained upon immersion of the PVA membranes in water for 30 min.

Surface Contact Angles of the Hydrogel. Surface contact angles (CA) of hydrogels were determined by using glycerol as the liquid phase in the absence and presence of a nonuniform magnetic field up to 0.08 T. The magnetic field was imposed by a neodymium magnet placed underneath the hydrogel membranes, and the magnetic field intensity was varied by adjusting the distance of the neodymium magnet to the hydrogel. The dynamic glycerol contact angles were determined in a sessile drop mode by using a drop shape analyzer system coupled to a video camera connected to a PC for data acquisition and the determination of the CA along time by using the CAM100 software. The final CA values were taken as the average of the values obtained for at least three replicates.

Protein Sorption Studies under Static and Dynamic Magnetic Field Conditions. Protein sorption experiments were conducted by immersion of PVA hydrogel membranes with different MNP loads in 1 g/L trypsin and FITC-albumin (only in dynamic field conditions) in a pH 8 Trizma buffer solution, in the absence and presence of magnetic field with different intensities up to 1 T. The supernatant was periodically sampled and analyzed by UV spectrophotometry at 280 nm to quantify the protein in the supernatant along time. The mass of protein sorbed (adsorbed and absorbed) in the hydrogel membrane in each moment was obtained by subtraction of the amount of protein in the initial solution by that present in the supernatant in the different sampling times.

Experiments at static magnetic field conditions were developed by keeping the magnetic field constant along the experiment time whereas dynamic magnetic field conditions were achieved by successively OFF/ON or ON/OFF magnetic field switching, where the magnetic field intensity was varied between 0 and 0.45 T or 1 T. Protein sorption studies at low magnetic field intensities (<0.5 T) were performed using a neodymium magnet, whereas a 3472 dipole H-frame electromagnet from GMW Associates (USA) was used to produce magnetic field intensities higher than 0.5 T. The H-frame electromagnet was coupled to a refrigeration bath for controlling the temperature of the magnetic poles. Both experimental setups were mounted in a way to ensure that the magnetic vector was perpendicularly oriented to the hydrogel surface.

Confocal Microscopy Measurements. Confocal fluorescence emission scans were acquired for hydrogel membranes used in FTIC-albumin sorption tests in the absence of magnetic field and exposed to OFF/ON magnetic field cycle by using a confocal laser scanning microscope (LSM 700/Carl Zeiss) with a 10 mW 488 nm laser.

DOI: 10.1021/acsami.9b03146
ACS Appl. Mater. Interfaces XXXX, XXX, XXX−XXX

Afterward, the image analysis was performed using ZEN 2.1 software (Carl Zeiss).

■ ASSOCIATED CONTENT

Supporting Information

The Supporting Information is available free of charge on the ACS Publications website at DOI: 10.1021/acsami.9b03146.

Tables S1−S3 and Figures S1−S4 (PDF)

■ AUTHOR INFORMATION

Corresponding Author

*(C.A.M.P.) E-mail cmp@fct.unl.pt; Ph +351 21 2948385.

ORCID

Carla A. M. Portugal: 0000-0003-0001-9265

Notes

The authors declare no competing financial interest.

■ ACKNOWLEDGMENTS

The authors acknowledge the financial support from Fundação para a Ciência e a Tecnologia (FCT-MEC), Portugal, through the projects EXPL/CTM-POL/1117/2012 and PTDC/EDM-EDM/30828/2017 and the PhD grant attributed to A.C.M. (SFRH/BD/114043/2015). This work was also supported by the LAQV-REQUIMTE, which is financed by national funds from FCT/MEC (UID/QUI/50006/2013) and cofinanced by the ERDF under the PT2020 Partnership Agreement (POCI-01-0145-FEDER-007265). The authors acknowledge Prof. Reyes Mallada (Univesity of Zaragoza, Spain) for access to the vibrating sample magnetometer (VSM) equipment and Dr. Pavel Strichovanec (Univesity of Zaragoza, Spain) for his technical assistance.

■ REFERENCES

(1) Wang, Y. N.; Tang, C. Y. Protein fouling of nanofiltration, reverse osmosis, and ultrafiltration membranes—The role of hydrodynamic conditions, solution chemistry, and membrane properties. *J. Membr. Sci.* **2011**, *376*, 275−282.

(2) Huisman, I. H.; Prádanos, P.; Hernández, A. The effect of protein−protein and protein−membrane interactions on membrane fouling in ultrafiltration. *J. Membr. Sci.* **2000**, *179*, 79−90.

(3) Yang, Q.; Himstedt, H.; Ulbricht, M.; Qian, X.; Wickramasinghe, S. R. Designing magnetic field responsive nanofiltration membranes. *J. Membr. Sci.* **2013**, *430*, 70−78.

(4) Gottschalk, U. Bioseparation in Antibody Manufacturing: The Good, The Bad and The Ugly. *Biotechnol. Prog.* **2008**, *24*, 496−503.

(5) Chopra, N.; Gavalas, V. G.; Bachas, L. G.; Hinds, B. J.; Bachas, L. G. Functional One-Dimensional Nanomaterials: Applications in Nanoscale Biosensors. *Anal. Lett.* **2007**, *40*, 2067−2096.

(6) Tokarev, I.; Tokareva, I.; Gopishetty, V.; Katz, E.; Minko, S. Specific Biochemical-to-Optical Signal Transduction by Responsive Thin Hydrogel Films Loaded with Noble Metal Nanoparticles. *Adv. Mater.* **2010**, *22*, 1412−1416.

(7) Wilson, C. J.; Clegg, R. E.; Leavesley, D. I.; Pearcy, M. J. Mediation of Biomaterial−Cell Interactions by Adsorbed Proteins: A Review. *Tissue Eng.* **2005**, *11*, 1−18.

(8) Stevens, M. M.; George, J. H. Exploring and Engineering the Cell Surface Interface. *Science* **2005**, *310*, 1135−1138.

(9) Gebreyohannes, A. Y.; Giorno, L.; Vankelecom, I. F.J.; Verbiest, T.; Aimar, P. Effect of operational parameters on the performance of a magnetic responsive biocatalytic membrane reactor. *Chem. Eng. J.* **2017**, *308*, 853−862.

(10) Chen, C. S. Mechanotransduction − a field pulling together? *J. Cell Sci.* **2008**, *121*, 3285−3292.

(11) Wang, Y.-X.; Robertson, J. L.; Spillman, W. B.; Claus, R. O. Effects of the Chemical Structure and the Surface Properties of Polymeric Biomaterials on Their Biocompatibility. *Pharm. Res.* **2004**, *21*, 1362.

(12) Irfan, M.; Idris, A. Overview of PES biocompatible/hemodialysis membranes: PES−blood interactions and modification techniques. *Mater. Sci. Eng., C* **2015**, *56*, 574−592.

(13) Guedidi, S.; Portugal, C. A.M.; Innocent, C.; Janot, J.-M.; Deratani, A.; Crespo, J. G. Fluorescence monitoring of trypsin adsorption in layer-by-layer membrane systems. *Enzyme Microb. Technol.* **2012**, *51*, 325−333.

(14) Nayak, A.; Liu, H.; Belfort, G. An Optically Reversible Switching Membrane Surface. *Angew. Chem., Int. Ed.* **2006**, *45*, 4094−4098.

(15) Roach, P.; Farrar, D.; Perry, C. C. Surface Tailoring for Controlled Protein Adsorption: Effect of Topography at the Nanometer Scale and Chemistry. *J. Am. Chem. Soc.* **2006**, *128*, 3939−3945.

(16) Grimaldi, J.; Radhakrishna, M.; Kumar, S. K.; Belfort, G. Stability of Proteins on Hydrophilic Surfaces. *Langmuir* **2015**, *31*, 1005−1010.

(17) Li, S.-S.; Xie, Y.; Xiang, T.; Ma, L.; He, C.; Sun, S.-D.; Zhao, C.-S. Heparin-mimicking polyethersulfone membranes − hemocompatibility, cytocompatibility, antifouling and antibacterial properties. *J. Membr. Sci.* **2016**, *498*, 135−146.

(18) Lei, J.; Ulbricht, M. Macroinitiator-mediated photoreactive coating of membrane surfaces with antifouling hydrogel layers. *J. Membr. Sci.* **2014**, *455*, 207−218.

(19) Lim, H. S.; Han, J. T.; Jin, D. K. M.; Cho, K. Photoreversibly switchable superhydrophobic surface with erasable and rewritable pattern. *J. Am. Chem. Soc.* **2006**, *128*, 14458−14459.

(20) Qi, H.; Cao, J.; Xin, Y.; Mao, X.; Xie, D.; Luo, J.; Chu, B. Dual responsive in hydrogel membrane with selective protein adsorption and sustained release property. *Mater. Sci. Eng., C* **2017**, *70*, 347−356.

(21) Wenzel, R. N. Resistance of solid surfaces to wetting by water. *Ind. Eng. Chem.* **1936**, *28*, 988−994.

(22) Cassie, A. B. D.; Baxter, S. Wettability of porous surfaces. *Trans. Faraday Soc.* **1944**, *40*, 546−561.

(23) Ross, A. M.; Jiang, Z.; Bastmeyer, M.; Lahann, J. Review: Physical Aspects of Cell Culture Substrates: Topography, Roughness, and Elasticity. Cell Culture Substrates. *Small* **2012**, *8*, 336−355.

(24) Sun, T.; Feng, L.; Gao, X.; Jiang, L. Bioinspired Surfaces with Special Wettability. *Acc. Chem. Res.* **2005**, *38*, 644−652.

(25) Zhang, X.; Shi, F.; Niu, J.; Jiang, Y.; Wang, Z. Superhydrophobic surfaces: from structural control to functional application. *J. Mater. Chem.* **2008**, *18*, 621−633.

(26) Seliktar, D. Designing Cell-Compatible Hydrogels for Biomedical Applications. *Science* **2012**, *336*, 1124−1128.

(27) Feinberg, A. W.; Feigel, A.; Shevkoplyas, S. S.; Sheehy, S.; Whitesides, G. M.; Parker, K. K. Muscular Thin Films for Building Actuators and Powering Devices. *Science* **2007**, *317*, 1366−1370.

(28) Chen, Y.-H.; Chung, Y.-C.; Wang, I.-J.; Young, T.-H. Control of cell attachment on pH-responsive chitosan surface by precise adjustment of medium pH. *Biomaterials* **2012**, *33*, 1336−1342.

(29) Patra, H. K.; Sharma, Y.; Islam, M. M.; Jafari, M. J.; Murugan, N. A.; Kobayashi, H.; Turner, A. P. F.; Tiwari, A. Inflammation-sensitive in situ smart scaffolding for regenerative medicine. *Nanoscale* **2016**, *8*, 17213−17222.

(30) Zhu, C.; Lu, Y.; Chen, J.; Yu, S. Photothermal Poly(*N*-isopropylacrylamide)/Fe_3O_4 Nanocomposite Hydrogel as a Movable Position Heating Source under Remote Control. Magnetic Hydrogels. *Small* **2014**, *10*, 2796−2800.

(31) Morales, D.; Bharti, B.; Dickey, M. D.; Velev, O. D. Bending of Responsive Hydrogel Sheets Guided by Field-Assembled Microparticle Endoskeleton Structures. Soft Actuators. *Small* **2016**, *12* (No.17), 2283−2290.

(32) Himstedt, H. H.; Qian, X.; Weaver, J. R.; Wickramasinghe, S. R. Responsive membranes for hydrophobic interaction chromatography. *J. Membr. Sci.* **2013**, *447*, 335−344.

DOI: 10.1021/acsami.9b03146
ACS Appl. Mater. Interfaces XXXX, XXX, XXX−XXX

(33) Xiao, L.; Isner, A.; Waldrop, K.; Saad, A.; Takigawa, D.; Bhattacharyya, D. Development of bench and full-scale temperature and pH responsive functionalized PVDF membranes with tunable properties. *J. Membr. Sci.* **2014**, *457*, 39−49.
(34) Nunes, S. P.; Behzad, A. R.; Hooghan, B.; Sougrat, R.; Karunakaran, M.; Pradeep, N.; Vainio, U.; Peinemann, K. Switchable pH-Responsive Polymeric Membranes Prepared via Block Copolymer Micelle Assembly. *ACS Nano* **2011**, *5*, 3516−3522.
(35) Szabó, D.; Szeghy, G.; Zrínyi, M. Shape Transition of Magnetic Field Sensitive Polymer Gels. *Macromolecules* **1998**, *31*, 6541−6548.
(36) Snyder, R. L.; Nguyen, V. Q.; Ramanujan, R. V. Design parameters for magneto-elastic soft Actuators. *Smart Mater. Struct.* **2010**, *19*, 055017.
(37) Fuhrer, R.; Athanassiou, E. K.; Luechinger, N. A.; Stark, W. J. Crosslinking Metal Nanoparticles into the Polymer Backbone of Hydrogels Enables Preparation of Soft, Magnetic Field-Driven Actuators with Muscle-Like Flexibility. *Small* **2009**, *5*, 383−388.
(38) Li, Y.; Huang, G.; Zhang, X.; Li, B.; Chen, Y.; Lu, T.; Lu, T. J.; Xu, F. Magnetic Hydrogels and Their Potential Biomedical Applications. *Adv. Funct. Mater.* **2013**, *23*, 660−672.
(39) Lin, X.; Quoc, B. N.; Ulbricht, M. Magnetoresponsive Poly(ether sulfone)-Based Iron Oxide cum Hydrogel Mixed Matrix Composite Membranes for Switchable Molecular Sieving. *ACS Appl. Mater. Interfaces* **2016**, *8*, 29001−29014.
(40) Willner, I.; Basnar, B.; Willner, B. From Molecular Machines to Microscale Motility of Objects: Application as "Smart Materials", Sensors, and Nanodevices. *Adv. Funct. Mater.* **2007**, *17*, 702−717.
(41) Sapir-Lekhovitser, Y.; Rotenberg, M. Y.; Jopp, J.; Friedman, G.; Polyak, B.; Cohen, S. Magnetically actuated tissue engineered scaffold: insights into mechanism of physical stimulation. *Nanoscale* **2016**, *8*, 3386−3399.
(42) Tognato, R.; Armiento, A. R.; Bonfrate, V.; Levato, R.; Malda, J.; Alini, M.; Eglin, D.; Giancane, G.; Serra, T. Stimuli-Responsive Nanocomposite for 3D Anisotropic Cell-Guidance and Magnetic Soft Robotics. *Adv. Funct. Mater.* **2019**, *29*, 1804647.
(43) Filipcsei, G.; Csetneki, I.; Szilágyi, A.; Zrínyi, M. Magnetic responsive-field smart polymer composites. *Adv. Polym. Sci.* **2007**, *206*, 137−189.
(44) Ge, J.; Hu, Y.; Biasini, M.; Beyermann, W. P.; Yin, Y. Superparamagnetic magnetite colloidal nanocrystal clusters. *Angew. Chem., Int. Ed.* **2007**, *46*, 4342−4345.
(45) Portugal, C. A. M. Functional membranes for the control of protein-surface interactions and transport properties. *Curr. Org. Chem.* **2017**, *21*, 1725−1739.
(46) Olle, B.; Bucak, S.; Holmes, T. C.; Bromberg, L.; Hatton, T. A.; Wang, D. I. C. Enhancement of Oxygen Mass Transfer Using Functionalized Magnetic Nanoparticles. *Ind. Eng. Chem. Res.* **2006**, *45*, 4355−4363.

DOI: 10.1021/acsami.9b03146
ACS Appl. Mater. Interfaces XXXX, XXX, XXX−XXX